











Article

Sesquiterpene Coumarin Ethers and Phenylpropanoids from the Roots of *Ferula drudeana*, the Putative Anatolian Ecotype of the Silphion Plant [†]

Fadil Kaan Kuran ^{1,2,3} , Sarath P. D. Senadeera ³ , Dongdong Wang ³ , Ji-Yeon Hwang ³ , Ekaterina Goncharova ^{3,4}, Jennifer Wilson ³ , Antony Wamiru ³, Brice A. P. Wilson ³ , Nathanael Pruett ⁵ , Lin Du ³ , Chuong D. Hoang ⁵, John A. Beutler ^{3,*}  and Mahmut Miski ^{1,*} 

- ¹ Department of Pharmacognosy, Faculty of Pharmacy, Istanbul University, Istanbul 34116, Türkiye; kaankuran@istanbul.edu.tr
- ² Department of Pharmacognosy, Institute of Graduate Studies in Health Sciences, Istanbul University, Istanbul 34116, Türkiye
- ³ Molecular Targets Program, National Cancer Institute, Frederick, MD 21702, USA; spdsenadeera@gmail.com (S.P.D.S.); dongdong.wang@nih.gov (D.W.); jiyeon.hwang@nih.gov (J.-Y.H.); katya.goncharova@nih.gov (E.G.); wilsonje@mail.nih.gov (J.W.); lin.du@nih.gov (L.D.)
- ⁴ Advanced Biomedical Computational Science, Frederick National Laboratory for Cancer Research, Frederick, MD 21702, USA
- ⁵ Thoracic Surgery Branch, National Cancer Institute, Bethesda, MD 20892, USA; chuong.hoang@nih.gov
- * Correspondence: beutlerj@mail.nih.gov (J.A.B.); mahmut.miski@gmail.com (M.M.)
- [†] The first author (F.K.K.) wishes to dedicate this paper to his father, Sözer Kuran, who passed away during the preparation of the manuscript and who supported his education in science.



Academic Editors: Francisco Leon, Xuefeng Wang and Maurizio Battino

Received: 7 March 2025

Revised: 15 April 2025

Accepted: 22 April 2025

Published: 25 April 2025

Citation: Kuran, F.K.; Senadeera, S.P.D.; Wang, D.; Hwang, J.-Y.; Goncharova, E.; Wilson, J.; Wamiru, A.; Wilson, B.A.P.; Pruett, N.; Du, L.; et al. Sesquiterpene Coumarin Ethers and Phenylpropanoids from the Roots of *Ferula drudeana*, the Putative Anatolian Ecotype of the Silphion Plant. *Molecules* **2025**, *30*, 1916. <https://doi.org/10.3390/molecules30091916>

Copyright: © 2025 by the authors. Licensee MDPI, Basel, Switzerland. This article is an open access article distributed under the terms and conditions of the Creative Commons Attribution (CC BY) license (<https://creativecommons.org/licenses/by/4.0/>).

Abstract: Four new sesquiterpene coumarin ethers (1–4) and a new phenylpropanoid compound (5) were isolated from a hexane extract of the roots of *Ferula drudeana*, the putative Anatolian ecotype of the silphion plant, in addition to nineteen previously described sesquiterpene coumarins (6–24) and four known phenylpropanoid derivatives (25–28). The structures of these compounds were elucidated by extensive spectroscopic analysis and computational studies. The cytotoxic activities of all isolated compounds were evaluated on renal, malignant pleural mesothelioma (MPM) and colon cancer cell lines. While 11 sesquiterpene coumarin derivatives showed strong-to-moderate cytotoxic activity against the UO31 renal cancer cell line, 13 compounds showed strong cytotoxic activity against the MPM cell line, and four sesquiterpene coumarin derivatives displayed moderate cytotoxic activity against the colon cancer cell line.

Keywords: Apiaceae; *Ferula drudeana*; sesquiterpene coumarin ethers; phenylpropanoid; kidney cancer

1. Introduction

The genus *Ferula*, with more than 227 species, is the largest genus of the Apiaceae family [1]. Many *Ferula* species have been used as medicinal plants since ancient times. Pedanius Dioscorides mentioned five drugs: Ammoniakon (*F. tingitana* or *F. marmarica*), Chalbane (*F. gummosis*), Narthex (*F. communis*), Sagapenon (*F. persica*), and Silphion, in his *De Materia Medica* [2]. Silphion (a.k.a., silphium) was a well-known medicinal resin mainly obtained from the roots of the silphion plant, most likely a *Ferula* species growing in the Cyrenaic region of Libya ca. 2300 years ago [3]. Pliny the Elder gives details of 39 remedies made with silphion in his “Natural History” [4]. Dioscorides describes the use of silphion to treat intestinal and hormonal disorders, goiter, sciatica, epilepsy, tetanus, polyps, and

malignant tumors [2]. However, silphion disappeared from commerce about the time of the Roman emperor Nero, after 500 years of robust trade around the Mediterranean [5].

Ferula drudeana Korovin, a rare and endemic species growing near former Greek villages in the Cappadocia region of Anatolia, was proposed as an Anatolian ecotype of the silphion plant due to its unusual morphological features and distinct organoleptic characteristics of its resin [6]. Similar to the descriptions of Theophrastus [7] and Pliny the Elder [4] for the silphion plant, *F. drudeana* has highly branched, thick roots that produce resin with a distinct aroma when an incision is made at the top of the root (Figure 1). Although it is possible to collect resin from the roots of *F. drudeana*, due to the scarce availability of live *F. drudeana* plants, we concluded that large-scale resin collection would endanger the survival of the species. The total amount of the resin collected from a limited number of plants would not be enough to investigate its secondary metabolites and their biological activity thoroughly. Therefore, hexane, dichloromethane, and methanol extracts of the roots of *F. drudeana* were prepared, and their secondary metabolite profile was compared with the resin. Since the secondary metabolite profile of the hexane extract of the roots of *F. drudeana* was almost identical to that of the resin (Supplementary Materials Figure S168), compounds were isolated from this extract and investigated for their biological activities.

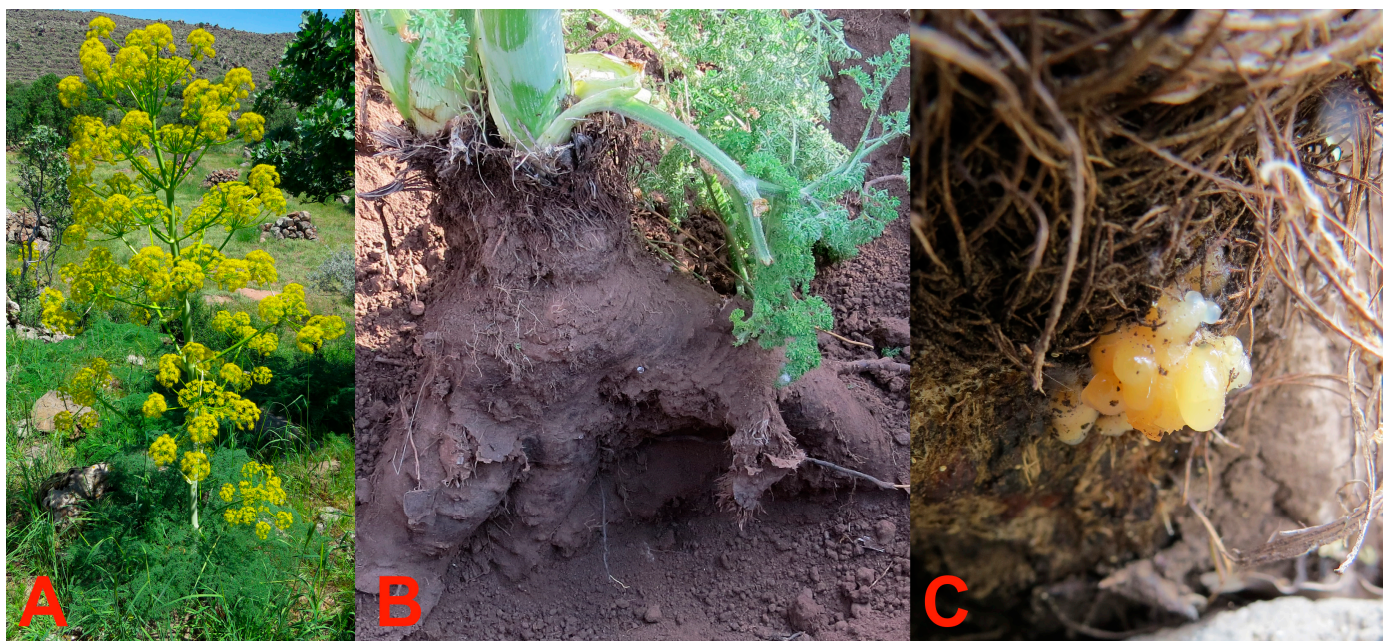


Figure 1. (A) The flowering stem of *Ferula drudeana*, (B) highly branched rhizomes of *F. drudeana*, (C) resin formation by solidification of the latex oozed from a small incision made at the top of the rhizome.

Here, we report the isolation and structure elucidation of the sesquiterpene coumarins and phenylpropanoids from the hexane extract of *Ferula drudeana* that may act as the active cytotoxic principles of silphion resin for the treatment of malignant tumors mentioned by Dioscorides [2].

2. Results

2.1. Characterization of Cytotoxic Compounds

The sesquiterpene coumarin derivatives and phenylpropanoids isolated from *F. drudeana* (Figure 2) were characterized through detailed spectroscopic and spectrometric analyses, including ^1H -NMR, ^{13}C -NMR, 2D NMR (HSQC, COSY, HMBC, NOESY), HRESIMS, IR, and UV-Vis.

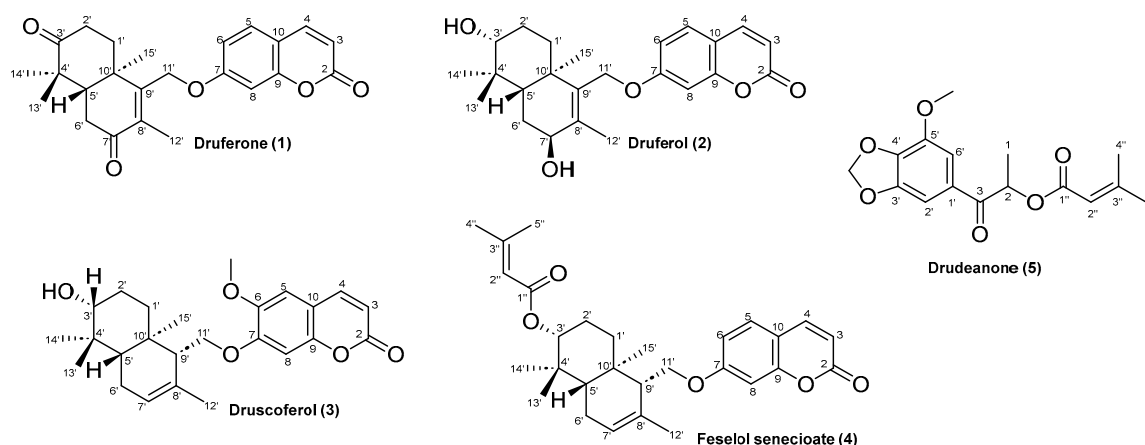


Figure 2. Structures of new compounds isolated from the roots of *F. drudeana*.

Druferone (**1**) was obtained as an amorphous white powder. The (+)-HRESIMS spectrum of **1** showed an $[M + H]^+$ molecular ion peak at m/z 395.1855, indicating a molecular formula of $C_{24}H_{26}O_5$. The 1H -NMR spectrum of **1** (Table 1) closely resembled that of the co-occurring ferubungeanol G (**13**) (Supplementary Materials Figures S2 and S60) [8]. A comparison of the 1H -NMR spectra between **1** and **13** (Supplementary Materials Figure S86) indicated the absence of the proton at the C3' position in **13**, accompanied by down-field shifts of some protons previously observed in the upfield region. The ^{13}C NMR spectrum of **1** (Supplementary Materials Figure S3) displayed a peak at δ_C 214.7, suggesting the presence of an additional carbonyl group compared to **13**. HMBC correlations from the deshielded protons H₂-2' at δ_H 2.70 and 2.52 to this carbonyl carbon signal (Figure 3a and Supplementary Materials Figure S6) indicated that the oxymethine at C-3' in **13** was oxidized to a carbonyl group in **1**. NOESY correlations observed for **1** (Figure 3b and Supplementary Materials Figure S7) validated its relative stereochemistry as 5'S*, 10'R*. The absolute configuration of **1** was determined to be 5'S, 10'R by good agreement of the experimental and calculated ECD spectra (Figure 3c).

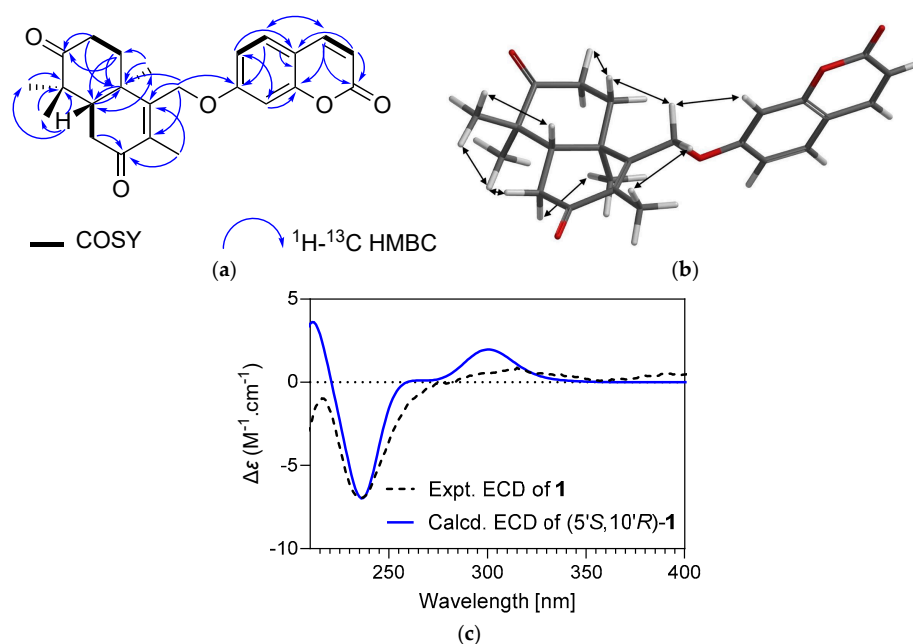


Figure 3. (a) COSY and HMBC correlations of **1**; (b) NOESY correlations of **1**; (c) experimental and calculated ECD spectra of **1**.

Druferol (**2**) was obtained as an amorphous white powder. The (+)-HRESIMS spectrum of **2** showed an $[M + H]^+$ ion peak at m/z 399.2180, confirming a molecular formula of $C_{24}H_{30}O_5$. Compound **2** exhibited close structural similarity to samarcandicin K (**14**) (Supplementary Materials Figures S11 and S62). The sole distinction between the two molecules lies in the stereochemistry of the hydroxyl group at C3'. The 1H -NMR spectral comparison between **2** and **14** (Supplementary Materials Figure S87) indicated a minor upfield shift in the resonance of H-3' in **2**, observed as a doublet of doublets with coupling constants of 11.6 and 4.2 Hz, which corroborated the assignment of H-3' to a β -axial position. Compound **2** was therefore determined to be the C3' epimeric form of **14**; NOESY correlations corroborate the stereochemical assignment illustrated in Figure 4b.

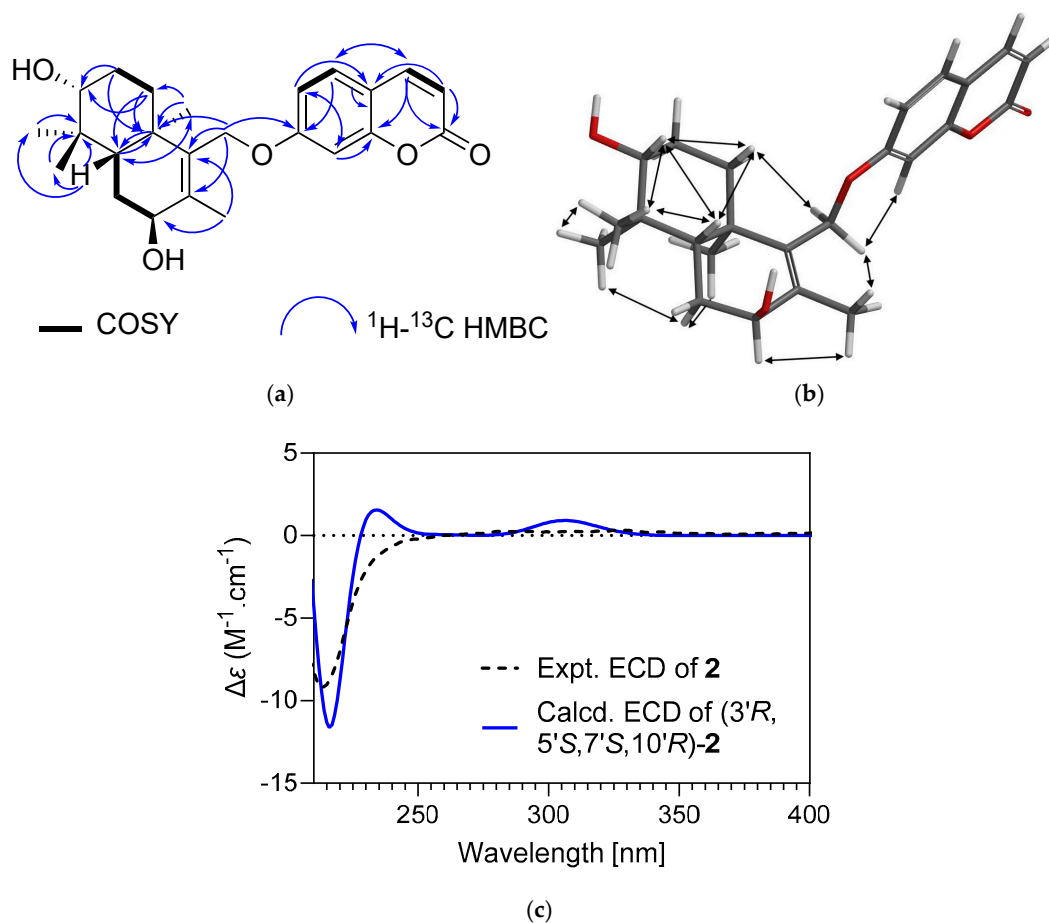


Figure 4. (a) Key COSY and HMBC correlations; (b) NOESY correlations; (c) experimental and calculated ECD spectra of **2**.

Druscoferol (**3**) was obtained as an amorphous white powder. The (+)-HRESIMS spectrum of **3** showed an $[M + H]^+$ ion peak at m/z 383.2219, suggesting a molecular formula of $C_{25}H_{32}O_5$ for **3**. The 1H -NMR spectrum of **3** (Table 1) showed high similarities to feselol (**11**), except for the absence of a 1,2,4-trisubstituted benzene ring and the presence of a 1,2,4,5-tetrasubstituted benzene ring and an additional methoxyl group (Supplemental Materials Figure S84). Detailed NMR analysis indicated that the H-6 in **11** was replaced by a methoxyl group in **3**. The assignment was supported by HMBC correlations from H-5, H-8, and 6-OCH₃ to C-6 (Figure 5a and Supplementary Materials Figure S24). The NOESY correlations of **3** (Supplementary Materials Figure S25) provided strong evidence that **3** had the same relative configuration as **11**.

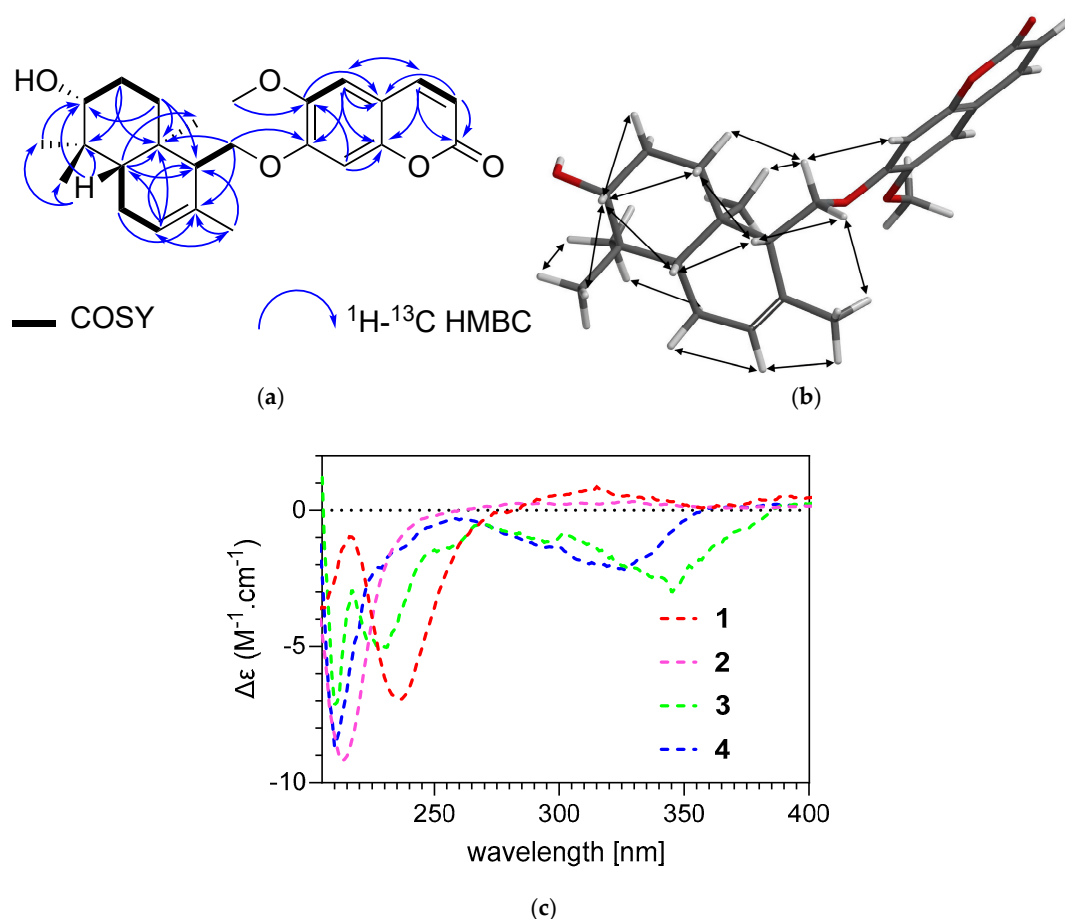


Figure 5. (a) Key COSY and HMBC correlations; (b) NOESY correlations; (c) experimental and calculated ECD spectra of 3 and 4 compared to 1 and 2.

The relative configurations of the drimane sesquiterpenoid skeleton at the C-5' and C-10' positions of **3** and **4** as (5'*S**,10*R**) were consistent with those of **1** and **2** based on the NOESY data. The absolute configurations of **1** and **2** were determined by comparison of their experimental and calculated ECD spectra. The ECD spectra of **3** and **4** showed a strong negative Cotton effect at ~215 nm, in combination with the biogenetic relationship, suggesting the same (5'*S*, 10*R*) absolute configuration of the drimane sesquiterpenoids as that of **1** and **2**. We also relied on our previous assignment of the absolute configuration of samarcandin by crystallography and ECD [8].

Fesolol senecioate (**4**) was obtained as an amorphous white powder. The (+)-HRESIMS spectrum of **4** showed an $[\text{M} + \text{Na}]^+$ ion peak at m/z 487.2460, revealing a molecular formula of $\text{C}_{29}\text{H}_{36}\text{O}_5$. The ^1H -NMR spectrum of **4** (Table 2) exhibited a notable resemblance to that of fesolol (**11**), except for the additional resonances for a senecioate substituent on 3 α -OH based on crucial HMBC correlations from two broad doublet methyls resonating at δ_{H} 2.17 and δ_{H} 1.89 to the olefinic carbons C-2'' (δ_{C} 116.7) and C-3'' (δ_{C} 156.3) and from H-3' and H-2'' (δ_{H} 5.68) to the senecioate carbonyl C-1'' (δ_{C} 166.5). The deshielded proton chemical shifts of 3'-methine (δ_{H} 4.57 in **4** vs. δ_{H} 3.27 in **11**) provided additional evidence for the esterification of this position. NOESY confirmed that its stereochemistry is the same as **11**. Accordingly, the fesolol senecioate (**4**) structure is proposed, as shown in Figure 6.

The relative configurations of the drimane sesquiterpenoid skeleton at the C-5' and C-10' positions of **3** and **4** as (5'*S**,10*R**) were consistent with those of **1** and **2** based on the NOESY data. The absolute configurations of **1** and **2** were determined by comparison of their experimental and calculated ECD spectra. The ECD spectra of **3** and **4** showed a strong negative Cotton effect at ~215 nm, in combination with the biogenetic relationship,

suggesting the same (5'S,10R) absolute configuration of the drimane sesquiterpenoids as that of **1** and **2**. We also relied on our previous assignment of the absolute configuration of samarcandin [8] by X-ray crystallography and ECD.

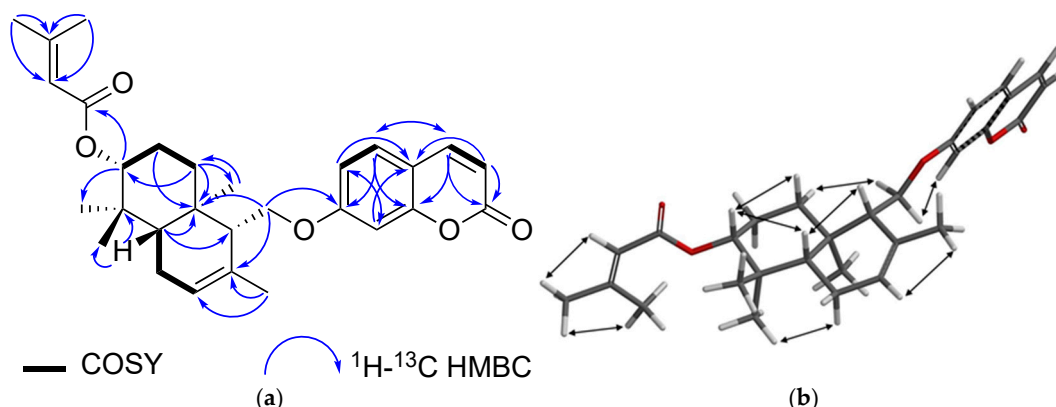


Figure 6. (a) Key COSY and HMBC correlations; (b) NOESY correlations of **4**.

As in the case of all drimane type of sesquiterpene coumarins, the sesquiterpene coumarins of *Ferula drudeana* were derived from the enzymatic cyclisation of umbelliprenin [or farnesyl ether of the corresponding coumarin derivative, e.g., druscoferol (**3**)] as their common precursor. Careful examination of the relative stereochemistries of sesquiterpene coumarins of *F. drudeana* (Figures 1 and 2) confirm the *cis* orientation of C-15'-methyl, C11'-methylene groups in the drimane skeleton. Since all known sesquiterpene coumarins' optical rotations were similar to those of published optical rotation data, this observation strongly suggests the absolute configurations of novel sesquiterpene coumarins as depicted in Figure 1, and the ECD data fully support this.

Drudeanone (**5**) was obtained as an amorphous white powder. The (+)-HRESIMS spectrum of **5** showed an $[M + H]^+$ ion peak at m/z 307.1182, corresponding to a molecular formula of $C_{16}H_{18}O_6$. The ¹H-NMR spectrum of **5** (Table 2) resembles that of crocatone (**26**), (Supplementary Materials Figure S88) except for the additional resonances for a senecioic acid substituent on C-2 to form an ester based on crucial HMBC correlations from two broad doublet methys resonating at δ_H 2.14 and δ_H 1.91 to the olefinic carbons C-2'' (δ_C 115.4) and C-3'' (δ_C 158.8) and from H-2 (δ_H 5.87, q, 7.0, 1H) and H-2'' (δ_H 5.80) to the senecionate carbonyl C-1'' (δ_C 165.9). Therefore, the structure of drudeanone (**5**) was determined as shown in Figure 7. Drudeanone did not show any optical rotation; therefore, it must be a racemic mixture of (+) and (−) isomers.

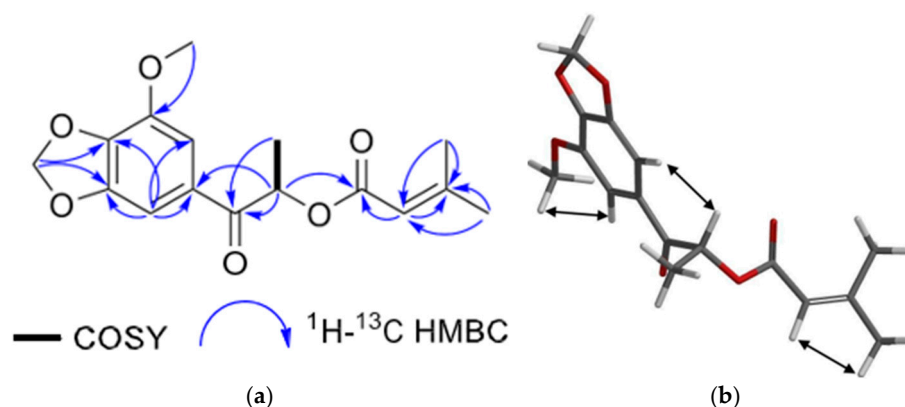
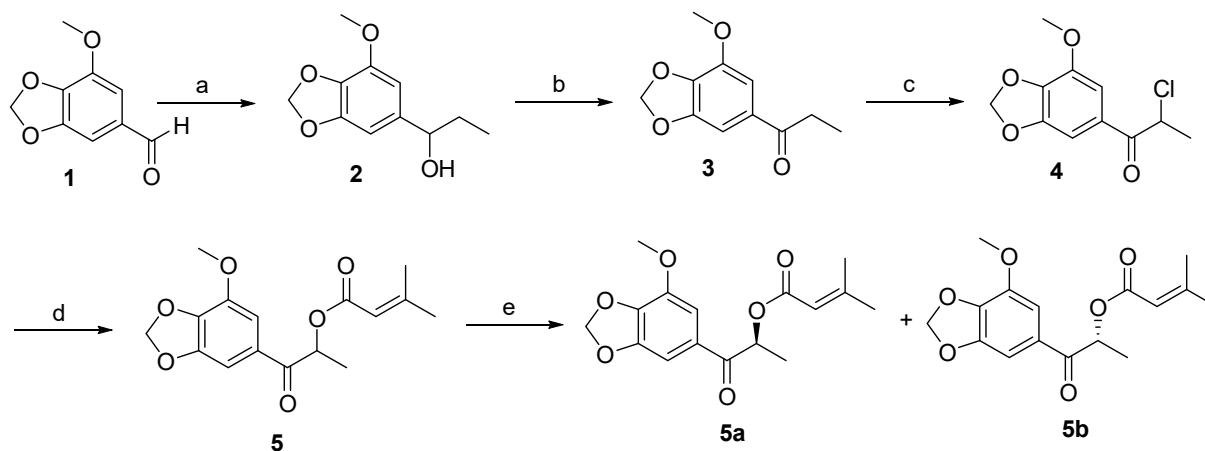


Figure 7. (a) Key COSY and HMBC correlations; (b) NOESY correlations of (**5**).

We proceeded to synthesize the compound **5** as shown in Scheme 1. Chiral HPLC provided both enantiomers **5a** and **5b**. DFT calculations of ECD (Figure 8) identified the respective absolute configurations, with **5a** being the *S*-enantiomer. These purified compounds showed opposite optical rotations, as would be expected.



Scheme 1. Synthesis and chiral separation of **5a** and **5b**.

Conditions: (a) ethylmagnesium bromide, THF, 0 °C to RT, 4 h; (b) PCC, DCM, RT, 4 h; (c) I₂, DMSO, 50 °C, 16 h; (d) 3-methylcrotonic acid, Et₃N, MeCN, 80 °C, 16 h; (e) chiral HPLC, Lux Cellulose-2.

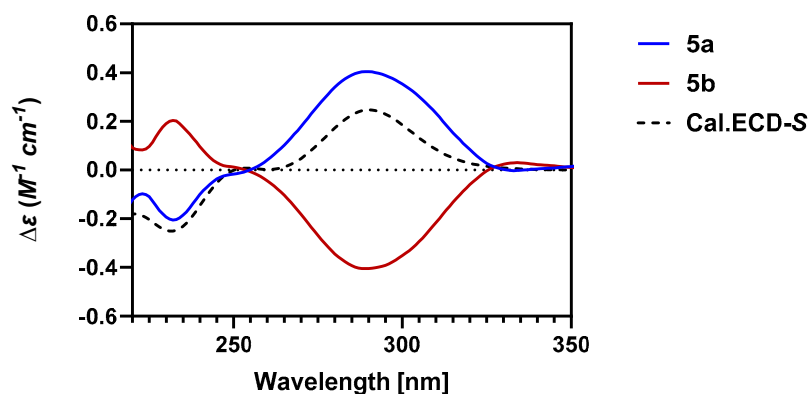


Figure 8. Comparison of the experimental and calculated ECD spectra for **5a** and **5b**.

Table 1. ¹H-NMR (600 MHz) and ¹³C-NMR (125 MHz) shifts of druferone (**1**), druferol (**2**), and druscoferol (**3**) (in CDCl₃, δ in ppm, and *J* in Hz).

Position	Druferone (1)		Druferol (2)		Druscoferol (3)	
	δ _H , Mult (<i>J</i> in Hz)	δ _C	δ _H , Mult (<i>J</i> in Hz)	δ _C	δ _H , Mult (<i>J</i> in Hz)	δ _C
2	-	161.1	-	161.6	-	161.8
3	6.29 (1H, d; 9.4)	113.8	6.25 (1H, d, 9.4)	113.5	6.26 (1H, d, 9.4)	113.7
4	7.64 (1H, d, 9.4)	143.4	7.64 (1H, d, 9.4)	143.8	7.60 (1H, d, 9.4)	143.7
5	7.41 (1H, d, 9.2)	129.1	7.37 1H, d, 9.2)	129.1	6.84 (1H, s)	109.1
6	6.85, m	113.2	6.86 (1H, dd, 9.2; 2.4)	113.4	-	147.3
7	-	161.5	-	162.9	-	152.8
8	6.86, m; 1H	101.5	6.84 (1H, d, 2.4)	101.7	6.82 (1H, s)	101.3
9	-	155.3	-	156.2	-	150.4
10	-	113.8	-	112.9	-	111.8

Table 1. Cont.

Position	Druferone (1)		Druferol (2)		Druscoferol (3)	
	δ_H , Mult (<i>J</i> in Hz)	δ_C	δ_H , Mult (<i>J</i> in Hz)	δ_C	δ_H , Mult (<i>J</i> in Hz)	δ_C
1' α	2.08, (2H, m)	34.3	1.71 (1H, m)	34.4	2.01 (1H, m)	37.9
1' β			1.49 (1H, br dd, 14.2, 5.07)		1.36 (1H, td, 13.0, 4.5)	
2' α	2.70 (1H, ddd, 15.8, 11.5, 7.0)	34.5	1.73 (1H, m)	27.8	1.64 (1H, ddd, 13.0, 3.5, 1.7)	27.7
2' β	2.52 (1H, m)		1.63 (1H, m)		1.66 (1H, m)	
3'	-	214.7	3.33 (1H, dd, 11.6, 4.2)	78.9	3.27 (1H, dd, 11.2, 4.4)	79.2
4'	-	47.2	-	39.0	-	39.1
5'	2.33 (1H, dd, 13.9, 4.0)	49.7	1.45 (1H, dd, 12.5, 2.6)	45.2	1.28 (1H, dd, 11.7, 5.1)	49.8
6' α	2.60 (1H, dd, 17.0, 13.9)	35.8	1.85–1.79 (2H, m)	28.7	2.02 (2H, m)	23.9
6' β	2.55 (1H, t, 4.58)					
7' α	-	199.3	4.08 (1H, br dd, 4.4, 1.7)	70.4	5.54 (2H, br s)	124.0
7' β	-		-			
8'	-	135.9	-	135.8	-	132.5
9'	-	154.3	-	139.4	2.32 (1H, dd, 6.8, 3.3)	53.9
10'	-	39.6	-	39.0	-	35.9
11' α	4.70 (1H, d, 9.9)	64.8	4.51 (1H, d, 9.84)	64.5	3.97 (1H, dd, 9.6, 6.8)	68.5
11' β	4.64 (1H, d, 9.9)		4.42 (1H, d, 9.84)		4.18 (1H, dd, 9.6, 3.3)	
12'	1.88 (3H, s)	12.0	1.83 (3H, s)	17.4	1.70 (3H, s)	21.9
13'	1.15 (3H, s)	21.4	1.00 (3H, s)	19.3	0.88 (3H, s)	15.1
14'	1.14 (3H, s)	26.0	0.84 (3H, s)	15.8	0.89 (3H, s)	15.6
15'	1.35 (3H, s)	18.4	1.06 (3H, s)	28.3	0.99 (3H, s)	28.4
-OCH ₃	-	-	-	-	3.85 (3H, s)	56.9

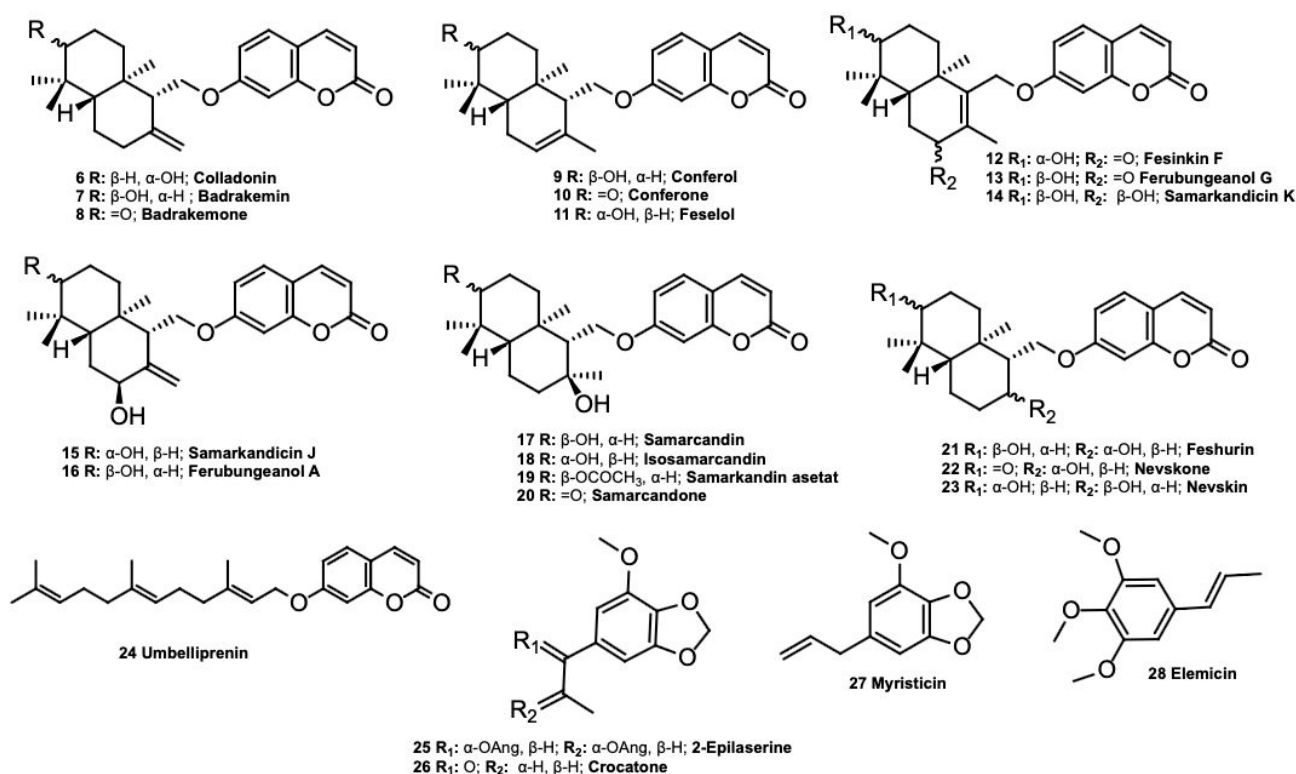
Table 2. 1H-NMR (600 MHz) and 13C-NMR (125 MHz) shifts of feselol senecioate (4) and drudeanone (5) (in CDCl₃, δ in ppm, and *J* in Hz).

Position	Feselol Senecioate (4)		Drudeanone (5)	
	δ_H , Mult (<i>J</i> in Hz)	δ_C	δ_H , Mult (<i>J</i> in Hz)	δ_C
1	-	-	1.51 (3H, d, 7.0)	17.5
2	-	161.1	5.87 (1H, q, 7.0)	70.5
3	6.24 (1H, d, 9.4)	112.9	-	195.4
4	7.63 (1H, d, 9.4)	143.3	-	-
5	7.36 (1H, d, 8.5)	128.6	-	-
6	6.82 (1H, dd, 8.5; 2.4)	113.0	-	-
7	-	161.8	-	-
8	6.80 (1H, d, 2.4)	101.5	-	-
9	-	155.8	-	-
10	-	112.4	-	-
1' α	2.02 (1H, m)		-	
1' β	1.42 (1H, dd, 13.5, 4.3)	37.4	-	140.3
2' α				
2' β	1.72 (2H, m)	34.5	7.15 (1H, d, 1.5)	103.1
3'	4.57 (1H, dd, 11.4, 4.3)	79.4	-	149.1
4'	-	37.5	-	140.3
5'	1.38 (1H, dd, 10.7; 5.7)	49.5	-	143.8
6' α				
6' β	2.02 (2H, m)	23.0	7.28 (1H, d, 1.5)	109.5
7'	5.55 (br d, 5.2)	123.5	-	-

Table 2. Cont.

Position	Fesolol Senecioate (4)		Drudeanone (5)	
	δ_H , Mult (J in Hz)	δ_C	δ_H , Mult (J in Hz)	δ_C
8'	-	132.2	-	-
9'	2.23 (1H, br s)	53.5	-	-
10'	-	35.5	-	-
11' α	4.16 (1H, dd, 9.7; 3.5)	-	-	-
11' β	4.01 (1H, dd 9.7; 5.7)	66.8	-	-
12'	1.69 (3H, br s)	21.5	-	-
13'	0.93 (3H, s)	14.7	-	-
14'	0.97 (3H, s)	16.4	-	-
15'	0.89 (3H, s)	27.9	-	-
1''	-	166.7	-	165.9
2''	5.68 (1H, d, 1.3)	116.7	5.8 (1H, br d, 1.3)	115.4
3''	-	156.3	-	158.8
4''	2.17; br d; 1.3; 3H	20.1	2.14 (3H, br d, 1.3)	20.5
5''	1.89; br d; 1.3; 3H	27.3	1.91 (3H, br d, 1.3)	27.6
-O-CH ₂ -O	-	-	6.06 (2H, br q, 1.5)	102.6
-O-CH ₃	-	-	3.93 (3H, s)	56.8

The known compounds colladonin (6) [9], badrakemin (7) [9], badrakemone (8) [8], conferol (9) [8], conferone (10) [8], fesolol (11) [8], fesinkin F (12) [10], ferubungeanol G (13) [10], samarcandicin K (14) [10], samarcandicin J (15) [10], ferubungeanol A (16) [10], samarcandin (17) [8], isosamarcandin (18) [11], samarcandin acetate (19) [8], samarcandone (20) [8], feshurin (21) [12], nevskone (22) [13], nevskin (23) [12], umbelliprenin (24) [14], 2-epilaserine (25) [15], crocatone (26) [16], myristicin (27) [17], and elemicin (28) [18] (Figure 9) were identified by comparison of their spectroscopic data with those of the literature data.

Figure 9. Known compounds isolated from *Ferula drudeana* roots.

A review of the biological activities of related known compounds suggests that several traditional medicinal applications of silphion, including anti-inflammatory, antiproliferative, antimycobacterial, immunomodulatory, selective estrogen receptor modulatory (e.g.,

aphrodisiac and emmenagogue), and cardioprotective effects, may be attributed to these compounds (Table 3).

Table 3. Biological activities of the known secondary metabolites of *Ferula drudeana*.

Secondary Metabolite	Biological Activities
Colladonin (6)	Cytotoxic against the COLO205 (colon), KM12 (colon), A498 (kidney carcinoma), UO31 (renal), TC32 (Ewing’s sarcoma) [19], HCT116 (human colorectal), HT-29 (human colorectal) [20], MCF-7, K-562 [11], A-549, U87MG, PC-3, and HEK293 [21] cancer cell lines, acetylcholinesterase (AChE) and butyrylcholinesterase (BChE) [22], carbonic anhydrase enzyme inhibition [23], endocannabinoid system modulator [24], α -amylase inhibition [25].
Badrakemin (7)	Cytotoxic against the KM12 (colon), A498 (kidney carcinoma), and UO31 (renal) cancer cell lines [19], acetylcholinesterase (AChE), butyrylcholinesterase (BChE), and tyrosinase (TYR) inhibition activity [22,26].
Badrakemone (8)	Cytotoxic against the UO31 (renal) [19], COLO205, K-562, MCF-7, HUVEC [8], A-549, U87MG, PC-3, and HEK293 [21] cancer cell lines, cancer chemoprevention [27], weak matrix metalloproteinase inhibitor [28], antiviral [10], anti-inflammatory [29], α -amylase inhibition [25].
Conferol (9)	Cytotoxic against the COLO205, K-562, MCF-7, and HUVEC [8] cell lines, urease inhibitor [30], modulators of multi-drug resistance in clinical isolates of <i>Escherichia coli</i> and <i>Staphylococcus aureus</i> [31], antileishmanial [32], antiviral against influenza A (H1N1) virus, cytotoxic against the HepG2 (hepatocellular carcinoma), Hep3B (hepatocellular carcinoma), and MCF-7 (estrogen-responsive mammalian adenocarcinoma) cancer cell lines [33].
Conferone (10)	Urease inhibitor [30], cytotoxic activity against the CH1 (ovarian), A549 (lung), SK-MEL-28 (melanoma) [34], COLO205, K-562, MCF-7 [8], and MT-2 [35] cell lines, cancer chemoprevention [27], antiviral [10].
Feselol (11)	Cytotoxic against COLO205, K-562, MCF-7, and HUVEC 7 [8], cancer chemoprevention [27], potential aphrodisiac [36], anti-inflammatory [27], antiviral [10].
Fesinkin F (12)	Cytotoxic against the HeLa cell line [10], antiviral [10], anti-inflammatory [27].
Ferubungeanol G (13)	Antiviral [10].
Samarcandicin K (14)	Antiviral [10].
Samarcandicin J (15)	Antiviral [10].
Samarcandin (17)	Potential aphrodisiac [36], antifungal [37], cytotoxic against the COLO205, K-562, MCF-7, HUVEC [8], AGS (human gastric carcinoma), and WEHI-164 (fibrosarcoma) cancer cell lines [38], active in NCI yeast anticancer drug-screen assays [39], potential antiviral activity against Ebola virus [40,41], antidiabetic [42], acetylcholinesterase (AChE) and carbonic anhydrase enzyme inhibition activity [23].
Isosamarcandin (18)	Cytotoxic against the COLO205, K-562, MCF-7, and HUVEC cancer cell lines [11], anti-inflammatory [29].
Samarcandin Acetate (19)	Potential aphrodisiac [36], cytotoxic against the COLO205, K-562, MCF-7, HUVEC [8] HeLa, and HT-29 cell lines [10], antiviral [10].
Samarcandone (20)	Anti-inflammatory [29], cytotoxic against the COLO205, K-562, MCF-7, and HUVEC cell lines [8].
Feshurin (21)	Cytotoxic against Mino cell line [43], antiviral [44].
Nevskin (23)	Cytotoxic against MV-4-11, Mino cell line [43].
Umbelliprenin (24)	Antigenotoxic [45], antioxidant, anti-inflammatory, lipoxygenase inhibitor [46], matrix metalloproteinase inhibitor [28], antitumor [47], cytotoxic activity against the CH1 (ovarian), A549 (lung), SK-MEL-28 (melanoma) [34], M4Beu (metastatic pigmented malignant melanoma), QU-DB (large cell lung) [48], COLO205, HCT116, A498 and UO31 (renal) [49], and MCF-7 [50] cancer cell lines, modulator of melanogenesis [51], antihypertension [52], cancer chemoprevention [27], antiangiogenic [53], antimetastatic and immunostimulatory [54], acetylcholinesterase (AChE) and carbonic anhydrase enzyme inhibition activity [23], antifungal [55], adjunctive agent for the treatment of pancreatic cancer [56], antineuroinflammatory, anxiolytic [57], anti-inflammatory effects by inhibiting TNF- α [58], butyrylcholinesterase (BChE) activity [22], antidiabetic [42].
2-Epilaserine (25)	Cytotoxicity against HL-60 cell line [15].
Crocatone (26)	Cytotoxicity against the HeLa and K562 cell lines [59], inhibition of abnormal proliferation of pulmonary artery smooth muscle cells (PASMCs) [60], spasmolytic [16], antifeedant [61].

Table 3. Cont.

Secondary Metabolite	Biological Activities
Myristicin (27)	Cancer chemopreventive agent [62], anti-inflammatory [63], antimicrobial against <i>B. subtilis</i> , <i>E. coli</i> , and <i>S. aureus</i> [64], hepatoprotective [65], cytoprotective against hypoxia-induced apoptosis and endoplasmic reticulum stress [66], downregulates expression of pro-inflammatory cytokines [67], cytotoxic against the SK-N-SH (human neuroblastoma) cancer cell line [68], antiproliferative [69], insecticidal against <i>Culex pipiens</i> and <i>Aedes aegypti</i> [70], antifungal [71], cytotoxic against MCF-7 [72], MAO inhibitory [73].
Elemicin (28)	Antifungal [71].

2.2. Cytotoxic Activity

The compounds isolated from *Ferula drudeana* were tested against kidney cancer cell lines (UO31 and A498) [74], mesothelioma cell lines representing two distinct histological subtypes of the disease MB24 (sarcomatoid) and MB52 (epithelioid) [75], together with a normal pleural mesothelial cell line NP1 [76] and a colon cancer cell line, (HCT116). The results are given in Table 4.

Table 4. IC₅₀ values of compounds isolated from *Ferula drudeana*.

Compound	IC ₅₀ (μM)					
	A498	UO31	MB24	MB52	NP1	HCT116
Druferone (1)	>50	>50	>30	29	28	>30
Druferol (2)	>50	>50	>30	>30	>30	>30
Druscoferol (3)	>50	35	18	18	20	27
Feselol senecioate (4)	>50	>50	>30	>30	>30	>30
Drudeanone (5)	>50	>50	>30	>30	>30	>30
Colladonin (6)	>50	33	25	29	24	>30
Badrakemin (7)	>50	39	>30	>30	>30	>30
Badrakemone (8)	>50	35	27	24	25	>30
Conferol (9)	>50	>50	24	>30	27	>30
Conferone (10)	>50	>50	>30	>30	>30	>30
Feselol (11)	>50	31	23	20	21	28
Fesinkin F (12)	NT *	NT	28	19	24	>30
Ferubungeanol G (13)	>50	39	22	17	15	26
Samarcandicin K (14)	>50	>50	>30	>30	>30	>30
Samarcandicin J (15)	>50	>50	>30	>30	>30	>30
Ferubungeanol A (16)	>50	22	22	30	14	>30
Samarcandin (17)	>50	43	>30	>30	>30	>30
Isosamarcandin (18)	NT	NT	25	8.5	15	>30
Samarcandin acetate (19)	>50	37	>30	>30	>30	>30
Samarcandone (20)	>50	>50	>30	>30	>30	>30
Feshurin (21)	>50	48	27	21	24	>30
Nevskone (22)	>50	>50	12	7.0	11	22
Umbelliprenin (24)	34	13	>30	>30	>30	>30
2-Epilaserine (25)	>50	>50	>30	>30	>30	>30
Crocatone (26)	>50	>50	>30	>30	>30	>30
Myristicin (27)	>50	>50	>30	>30	>30	>30
Elemicin (28)	>50	>50	>30	>30	>30	>30

* NT = Not tested.

3. Discussion

In continuation of our preliminary study on the secondary metabolites of *F. drudeana* [77], an endemic species of Türkiye, subsequent isolation studies performed on the hexane extract of the roots of *F. drudeana* led to the identification of 23 sesquiterpene coumarin ethers and five phenylpropanoid derivatives. These molecules were evaluated for their cytotoxic activities using cell growth assays on kidney cancer cell lines (UO31, A498), DPM

cell lines (MB52 and MB24), together with a normal pleural mesothelial cell line (NP1), and one colon cancer cell line (HCT116).

The results of cytotoxicity assays demonstrate that umbelliprenin (**24**) is the most cytotoxic molecule to kidney cancer cell lines, exhibiting IC_{50} values of 34 μ M and 13 μ M against A498 and UO31, respectively, but it showed no cytotoxicity in any of the other tested cell lines. Ferubungeanol A (**16**) exhibited considerable cytotoxicity against MPM cell lines, with IC_{50} values of 30 μ M on MB52, 14 μ M on NP1, and 22 μ M on MB24.

The results of cytotoxicity assays demonstrate that umbelliprenin (**24**) is the most cytotoxic molecule to kidney cancer cell lines, exhibiting IC_{50} values of 34 μ M and 13 μ M against A498 and UO31, respectively, but it showed no cytotoxicity in any of the other tested cell lines. Ferubungeanol A (**16**) exhibited considerable cytotoxicity against MPM cell lines, with IC_{50} values of 30 μ M on MB52, 14 μ M on NP1, and 22 μ M on MB24.

Ferubungeanol A (**16**) also demonstrated notable cytotoxicity against the UO31 cell line, with an IC_{50} value of 22 μ M. Structurally, ferubungeanol A (**16**) is a derivative of badrakemin (**7**), bearing a hydroxyl group at the C-7' position. In contrast, badrakemin (**7**) exhibited cytotoxic activity only against the UO31 cell line, with an IC_{50} value of 39 μ M, and showed no activity against other cell lines. These findings suggested that the hydroxyl group at the C-7' position plays a crucial role in enhancing the cytotoxic activity, highlighting its importance in structure-activity relationships.

Colladonin (**6**) is the C-3' epimer of badrakemin (**7**). Although epimerization slightly enhances the activity of colladonin (**6**) against the cell lines, the comparable activity levels between colladonin (**6**) and badrakemin (**7**) suggest that this structural modification does not appreciably affect their cytotoxic potential. A comparable example can be observed with the molecules feselol (**11**) and conferol (**9**), which are also C-3' epimers. The relationship between their activities mirrored that of colladonin (**6**) and badrakemin (**7**), further supporting the limited impact of C-3' epimerization on cytotoxic activity. Samarcandin (**17**) and isosamarcandin (**18**) are also C-3' epimers. In contrast to the colladonin-badrakemin and feselol-conferol epimer pairs, a noteworthy difference in cytotoxic activity is observed in the samarcandin-isosamarcandin epimer pair. While samarcandin (**17**) exhibited no cytotoxic activity against any tested cell lines, isosamarcandin (**18**) showed activity against MB52 (8.5 μ M), NP1 (15 μ M), and MB24 (25 μ M) cell lines. The results indicate that the α -configuration of the hydroxyl group at the C-3' position in isosamarcandin (**18**) significantly enhanced its cytotoxic activity, and these findings underscore the critical role of the α -hydroxyl group at the C-3' position in modulating cytotoxic activity.

Druscoferol (**3**), a novel compound isolated from the roots of *Ferula drudeana*, is a derivative of feselol (**11**), wherein the coumarin moiety is scopoletin rather than umbelliferone. A comparison of the cytotoxic activities of druscoferol (**3**) and feselol (**11**) across all tested cell lines revealed highly similar results. Druscoferol (**3**) exhibited cytotoxicity against MB52 (IC_{50} : 18 μ M), MB24 (IC_{50} : 18 μ M), NP1 (IC_{50} : 20 μ M), HCT116 (IC_{50} : 24 μ M), and UO31 (IC_{50} : 5.0 μ M) cell lines, demonstrating an activity profile comparable to that of feselol (**11**). These findings suggest that methoxy substitution of the coumarin moiety does not significantly affect the cytotoxic activity of these compounds across the tested cell lines. Ferubungeanol G (**13**) emerged as another notable cytotoxic sesquiterpene coumarin, demonstrating activity, particularly against MB52 (IC_{50} : 17 μ M), NP1 (IC_{50} : 15 μ M), MB24 (IC_{50} : 22 μ M), and HCT116 (IC_{50} : 26 μ M) cell lines. The cytotoxic activity of feshurin (**21**), the C-8' epimer of samarcandin (**17**), exhibited significant cytotoxicity in certain cell lines. Conversely, samarcandone (**20**), a derivative formed by oxidation of the hydroxyl group at the C-3' position of samarcandin (**17**) into a ketone, showed no cytotoxic activity in any tested cell lines. Nevskone (**22**), the ketone derivative of feshurin (**21**), exhibited substan-

tial cytotoxicity in specific cell lines. These results demonstrate that configurational and substitutional differences significantly influence the cytotoxic activity of these molecules.

4. Materials and Methods

4.1. General Experimental Procedures

LC-MS analyses were carried out using an 6130 Quadrupole LC/MS system (Agilent Technologies®, Santa Clara, CA, USA). UV-Vis spectra were recorded with a Nanodrop 2000 C (Thermo Scientific, Waltham, MA, USA) using a 1 mm quartz cuvette. IR spectra were measured on a Alpha FT-IR spectrometer (Bruker®, Billerica, MA, USA). NMR spectra were obtained using a Bruker® Avance III spectrometer operating at 600 MHz for ^1H and 150 MHz for ^{13}C , respectively, with deuterated chloroform as the solvent. High-resolution electrospray ionization mass spectrometry (HRESIMS) data were collected with an Agilent® 6530 Accurate Mass Q-TOF instrument. Optical rotation measurements were performed on a Autopol V Plus® polarimeter using dichloromethane or methanol as the solvent (Rudolph Analytical, Hackettstown, NJ, USA). Initial fractionation was conducted using a Sephadex LH-20 column (5×100 cm, 25–100 μm , (Sigma Chem. Co., GE Healthcare, Chicago, IL, USA). Further purification of the compounds was achieved using a HPLC 2050 system (Gilson®, Saint-Avé, France). Chromatographic procedures utilized solvents, including hexane, dichloromethane, methanol, and acetonitrile, which were purchased from Sigma-Aldrich.

4.2. Plant Material

The plant material used in this study was collected from Mount Hasan in Aksaray Province, Türkiye, on 28 May 2019. The plant material was identified as *Ferula drudeana* Korovin by Professors Emine Akalin and Mahmut Miski. The herbarium specimen was archived in the herbarium of Istanbul University Faculty of Pharmacy (ISTE 115986).

4.3. Extraction and Isolation

The dried and coarsely powdered roots (900 g) of *F. drudeana* were extracted by maceration at room temperature with hexane (2×1 L) for 1 h in a Soxhlet extractor. After maceration, the plant material was further subjected to continuous extraction with hexane to extract medium-polar compounds such as sesquiterpene coumarins and phenyl propanoids. The solvent was evaporated under reduced pressure in a rotary evaporator at 35 °C, and a hexane extract of ca. 28 g was obtained, which was subjected to a silica (0.2–0.5 mm) open column to obtain 18 fractions. Each fraction was checked with LC-MS and combined to yield 10 fractions. Fractions that contain sesquiterpene coumarins and phenyl propanoids were fractionated on a Sephadex LH-20 column (5×100 cm) using a mobile-phase (hexane: dichloromethane: methanol with 7:4:1) solvent system. The secondary metabolite profile of each fraction was examined by LC-MS, and similar fractions were combined to yield 30 fractions. All fractions that were more than 20 mg were further purified on a reverse-phase preparative HPLC with gradient elution at a flow rate of 9 mL/min for 70 min. Fractions with less than 20 mg were subjected to reverse-phase semi-preparative HPLC purification at a flow rate of 4 mL/min for 70 min. During HPLC purification, chromatograms were observed at 200–600 nm, 210 nm, 254 nm, 280 nm, and 366 nm wavelengths. Phenomenex® Luna C₁₈ columns (21.2×150 mm and 10×250 mm) were used for purification. Acetonitrile and water were used as the mobile phase. The mobile phase systems were modified based on the characteristics of fractions.

Druferone (**1**): Amorphous white powder, $[\alpha]_D^{24}$: -11° (c, 0.4, MeOH); UV (c, 0.015 mg/mL) (MeOH) λ_{max} (log ϵ) nm: 247 (sh) (4.09), 324 (4.09). IR ν_{max} (cm^{-1}):

2959, 2920, 2850, 1734, 1707. ^1H - and ^{13}C -NMR, see Table 1. HRESIMS m/z $[\text{M} + \text{H}]^+$ 395.1855 (calculated for $\text{C}_{24}\text{H}_{27}\text{O}_5$: 395.1853).

Druferol (2): Amorphous white powder, $[\alpha]^{24}_{\text{D}}$: -24° (c, 2.0, MeOH); UV (c, 0.015 mg/mL) (MeOH) λ_{max} (log ϵ) nm: 202 (4.58), 327 (4.07). IR ν_{max} (cm^{-1}): 3431, 3085, 2959, 2930, 2869, 1728. ^1H - and ^{13}C -NMR data, see Table 1. HRESIMS m/z $[\text{M} + \text{H}]^+$ 399.2180 (calculated for $\text{C}_{24}\text{H}_{31}\text{O}_5$: 399.2166).

Druscoferol (3): Amorphous white powder, $[\alpha]^{24}_{\text{D}}$: -55.91° (c, 8.5, MeOH); UV (c, 0.015 mg/mL) (MeOH) λ_{max} (log ϵ) nm: 232 (4.75), 299 (sh) (4.29), 345 (4.56). IR ν_{max} (cm^{-1}): 3461, 3083, 2960, 2932, 2854, 1718. ^1H - and ^{13}C -NMR data, see Table 1. HRESIMS m/z $[\text{M} + \text{H}]^+$ 413.2336 (calculated for $\text{C}_{25}\text{H}_{33}\text{O}_5$: 413.2323).

Feselol senecioate (4): Amorphous white powder, $[\alpha]^{24}_{\text{D}}$: -107.06° (c, 3.4, MeOH); UV (c, 0.015 mg/mL) (MeOH) λ_{max} (log ϵ) nm: 220 (sh) (4.45), 326 (4.12). IR ν_{max} (cm^{-1}): 3082, 2969, 2940, 2923, 2853, 1735. ^1H - and ^{13}C -NMR data, see Table 2. HRESIMS m/z $[\text{M} + \text{Na}]^+$ 487.2460 (calculated for $\text{C}_{29}\text{H}_{36}\text{O}_5\text{Na}$: 487.2455).

Drudeanone (5): Amorphous white powder, $[\alpha]^{24}_{\text{D}}$: 0° (c, 3.5, MeOH); UV (c, 0.02 mg/mL) (MeOH) λ_{max} (log ϵ) nm: 212 (5.23), 304 (4.52). FT-IR ν_{max} (cm^{-1}): 2939, 1694. ^1H - and ^{13}C -NMR data, see Table 2. HRESIMS m/z $[\text{M} + \text{H}]^+$ 307.1182 (calculated for $\text{C}_{16}\text{H}_{18}\text{O}_6$: 307.1181).

4.4. Cytotoxic Activity Studies

The XTT bioactivity test is an in vitro colorimetric cytotoxic activity test developed by the NCI MTP Assay Development and Screening Section [74] and used for this study. Kidney (A498, UO31) and colon (HCT116) cancer cell lines were used during the tests. These cell lines were obtained from the NCI Developmental Therapeutics Program. RPMI-1640 (Roswell Park Memorial Institute, Buffalo, NY, USA) medium, 10% FBS (fetal bovine serum), 1% glutamine, and 1% penicillin/streptomycin solutions were used for cell growth and treatment. Transfers were performed under laminar airflow in a sterile environment. The suspension containing the cells was seeded into 384-well plates with a volume of 45 μL with 3.5×10^5 cells per well. Then, the plate was incubated at 37°C and 5% CO_2 for 24 h. The pure compounds prepared in DMSO were added in a 10-concentration series and incubated for another 48 h. After incubation, 10 μL of the tetrazolium salt XTT (2,3-bis [2-methoxy-4-nitro-5-sulphophenyl]-2H-tetrazolium-5-carboxanilide) solution was applied to the cells. After 4 h of incubation, dead cells were not stained with formazan dye, while viable cells could be counted in the EnVision plate reader using UV absorbance at 450 nm and 650 nm. Sanguinarine chloride hydrate was used as a positive control in the experiment. All assays involved duplicate wells for each sample concentration.

The other cytotoxicity assay was performed on diffuse pleural mesothelioma (DPM) cell lines representing two distinct histological subtypes of the disease MB52 (epithelioid) and MB24 (sarcomatoid) as well as NP1, a normal pleural mesothelioma cell line for comparison. This assay was developed by the National Cancer Institute, Thoracic Surgery Branch, Bethesda, and the methodologies for generating the NP1, MB24, and MB52 cell lines have been published [75,76], respectively. For this assay, the molecules were dissolved in DMSO and prepared at a stock concentration of 6 mM. The stock solution was diluted 200-fold to achieve an initial test concentration of 30 μM , and growth was assessed at 72 h. Sanguinarine chloride hydrate was also used as a positive control in the experiment, with an IC_{50} value of 1 μM for all three cell lines. All assays involved duplicate wells for each sample concentration.

4.5. Computational Details

Conformational searches were performed in an energy window of 5 kcal/mol using MacroModel, Schrödinger 2024 for **1** and **2**. The low-energy conformers were optimized with Gaussian 16 using DFT/B3LYP/DGDZVP in MeOH for **1** and **2**. The optimized conformers with Boltzmann distributions (%) greater than 1% were further submitted to the ECD calculation to generate the simulated ECD spectra using TDDFT/M062X/DGDZVP in MeOH for **1**. The calculated ECD spectra were further averaged based on the Boltzmann distributions to afford the theoretical ECD spectra for **1**.

5. Conclusions

This study represents the first comprehensive isolation study on the roots of *Ferula drudeana*, an endemic species of Türkiye. A total of 28 compounds were isolated, and their cytotoxic activities were evaluated using cell-based assays developed at the National Cancer Institute. As a result, 11 of the sesquiterpene coumarin derivatives demonstrated measurable cytotoxicity.

Supplementary Materials: The following supporting information can be downloaded at <https://www.mdpi.com/article/10.3390/molecules30091916/s1>, Figure S1–S168. Spectroscopic data for compounds, detailed biological results, comparative HPLC traces for hexane extract of root and resin, and synthesis of compound **5**; Table S1. DFT/B3LYP/DGDZVP optimized conformers of model structure **5a** submitted for ECD simulations at TDDFT/B3LYP/DGDZVP in gas phase. Reference [78].

Author Contributions: Conceptualization, M.M. and J.A.B.; methodology, F.K.K., C.D.H. and S.P.D.S.; software, F.K.K., S.P.D.S., E.G. and M.M.; validation, F.K.K., S.P.D.S., A.W., N.P., E.G., J.A.B. and M.M.; formal analysis, F.K.K., S.P.D.S., J.W., J.A.B., B.A.P.W. and M.M.; investigation, F.K.K., S.P.D.S., D.W., J.W., L.D., J.-Y.H., A.W., N.P., B.A.P.W., J.A.B. and M.M.; resources, F.K.K., S.P.D.S., J.A.B. and M.M.; data curation and writing—original draft preparation, F.K.K. and M.M.; writing—review and editing, F.K.K., S.P.D.S., D.W., J.A.B. and M.M.; visualization, F.K.K. and M.M.; supervision, L.D., C.D.H., M.M. and J.A.B.; project administration, F.K.K., S.P.D.S., J.A.B. and M.M.; funding acquisition, C.D.H., L.D. and J.A.B. All authors have read and agreed to the published version of the manuscript.

Funding: This research was funded by the Scientific Research Projects Coordination Unit of Istanbul University, project number TDK-2020-36825. This study is supported by 2214-A programme of the Scientific and Technological Research Council of Turkey (TÜBİTAK). This research was also supported in part by the Intramural Research Program of the NIH, National Cancer Institute, Center for Cancer Research (ZIABC011470 and ZIABC011657), and with federal funds from the National Cancer Institute, National Institutes of Health, under contract 75N91019D00024. The content of this publication does not necessarily reflect the views or policies of the Department of Health and Human Services, nor does mention of trade names, commercial products, or organizations imply endorsement by the U.S. Government.

Institutional Review Board Statement: Not applicable.

Informed Consent Statement: Not applicable.

Data Availability Statement: Data is available on request to the corresponding authors.

Conflicts of Interest: The authors declare no conflicts of interest.

References

1. Plants of the World Online (POWO). *Ferula* L. Available online: <https://powo.science.kew.org/taxon/30105171-2#publications> (accessed on 15 February 2025).
2. Gunther, R.T. *The Greek Herbal of Dioscorides*; Hafner Press: Royal Oak, MI, USA, 1959.
3. Gemmill, C.L. Silphium. *Bull. Hist. Med.* **1966**, *40*, 295–313. [PubMed]

4. Bostock, J.; Riley, H. Book XIX, The Nature and Cultivation of Flax, and an Account of Various Garden Plants, Chapter 15, Laserpitium, Laser and Maspetuem. Book XXII, The Properties of Plants and Fruits, Chapter 49; Laser: Thirty-nine Remedies. In *Pliny the Elder, Natural History; Collected Works of Pliny the Elder; Delphi Classics*; Delphi Publishing Ltd.: Hastings, UK, 2015.
5. Amigues, S. Le silphium—État de la question. *J. Des. Savants* **2004**, *2*, 191–226. [[CrossRef](#)]
6. Miski, M. Next chapter in the legend of silphion: Preliminary morphological, chemical, biological and pharmacological evaluations, initial conservation studies, and reassessment of the regional extinction event. *Plants* **2021**, *10*, 102. [[CrossRef](#)] [[PubMed](#)]
7. Hort, A. Book VI of *Under-Shrubs* [3.2–3.4]; Theophrastus, Enquiry into Plants; Collected Works of Theophrastus; Delphi Publishing Ltd., Delphi Classics, Hastings: East Sussex, UK, 2019.
8. Eruçar, F.M.; Kuran, F.K.; Altıparmak, Ü.G.; Özbey, S.; Karavuş, Ş.N.; Arcan, G.G.; Yazıcı Tütüniş, S.; Tan, N.; Aksoy Sağırılı, P.; Miski, M. Sesquiterpene coumarin ethers with selective cytotoxic activities from the roots of *Ferula huber-morathii* Peşmen (Apiaceae) and unequivocal determination of the absolute stereochemistry of samarcandin. *Pharmaceuticals* **2023**, *16*, 792. [[CrossRef](#)]
9. Tosun, F.; Aytar, E.; Beutler, J.; Wilson, J.; Miski, M. Cytotoxic sesquiterpene coumarins from the roots of *Heptaptera cilicica*. *Rec. Nat. Prod.* **2021**, *15*, 529–536. [[CrossRef](#)]
10. Zhang, M.-M.; Kamoldinov, K.; Nueraihemaiti, M.; Turdu, G.; Zou, G.-A.; Aisa, H.A. Sesquiterpene coumarins with anti-vitiligo and cytotoxic activities from *Ferula samarkandica*. *Phytochem. Lett.* **2024**, *61*, 21–28. [[CrossRef](#)]
11. Kuran, F.K.; Altıparmak, Ü.G.; Arcan, G.G.; Eruçar, F.M.; Karavuş, Ş.N.; Aksoy Sağırılı, P.; Tan, N.; Miski, M. Sesquiterpene coumarins, chromones, and acetophenone derivatives with selective cytotoxicities from the roots of *Ferula caspica* M. Bieb. (Apiaceae). *Pharmaceuticals* **2024**, *17*, 1254. [[CrossRef](#)]
12. Tashkhodzhaev, B.; Turgunov, K.K.; Izotova, L.Y.; Kamoldinov, K.S. Stereochemistry of samarcandin-type sesquiterpenoid coumarins. Crystal structures of feshurin and nevskin. *Chem. Nat. Compd.* **2015**, *51*, 242–246. [[CrossRef](#)]
13. Bagirov, V.Y. A coumarin from the roots of *Ferula nevskii*. *Chem. Nat. Compd.* **1978**, *14*, 562. [[CrossRef](#)]
14. Iranshahi, M.; Gholam-Reza, A.; Hassan, J.; Shafiee, A. New germacrane derivative from *Ferula persica*. *Pharm. Biol.* **2003**, *41*, 431–433. [[CrossRef](#)]
15. Yang, R.-L.; Yan, Z.-H.; Lu, Y. Cytotoxic phenylpropanoids from carrot. *J. Agric. Food Chem.* **2008**, *56*, 3024–3027. [[CrossRef](#)] [[PubMed](#)]
16. Pavlović, I.; Krunić, A.; Nikolić, D.; Radenković, M.; Branković, S.; Niketić, M.; Petrović, S. Chloroform Extract of Underground Parts of *Ferula heuffelii*: Secondary Metabolites and Spasmolytic Activity. *Chem. Biodivers.* **2014**, *11*, 1417–1427. [[CrossRef](#)] [[PubMed](#)]
17. You, C.X.; Jiang, H.Y.; Zhang, W.J.; Guo, S.S.; Yang, K.; Lei, N.; Ma, P.; Geng, Z.F.; Du, S.S. Contact toxicity and repellency of the main components from the essential oil of *Clausena anisum-olens* against two stored product insects. *J. Insect Sci.* **2015**, *15*, 87. [[CrossRef](#)]
18. Rossi, P.-G.; Bao, L.; Luciani, A.; Panighi, J.; Desjobert, J.-M.; Costa, J.; Casanova, J.; Bolla, J.-M.; Berti, L. (E)-Methylisoeugenol and elemicin: Antibacterial components of *Daucus carota* L. essential oil against *Campylobacter jejuni*. *J. Agric. Food Chem.* **2007**, *55*, 7332–7336. [[CrossRef](#)]
19. Tosun, F.; Beutler, J.A.; Ransom, T.T.; Miski, M. Anaticin, a Highly Potent and Selective Cytotoxic Sesquiterpene Coumarin from the Root Extract of *Heptaptera anatolica*. *Molecules* **2019**, *24*, 1153. [[CrossRef](#)] [[PubMed](#)]
20. Jabrane, A.; Jannet, H.B.; Mighri, Z.; Mirjolet, J.-F.; Duchamp, O.; Harzallah-Skhiri, F.; Lacaille-Dubois, M.-A. Two New Sesquiterpene Derivatives from the Tunisian Endemic *Ferula tunetana* Pom. *Chem. Biodivers.* **2010**, *7*, 392–399. [[CrossRef](#)] [[PubMed](#)]
21. Tosun, F.; Biltekin, S.; Karadağ, A.; Mihoglugil, F.; Akalgan, D.; Miski, M. Biological activities of the natural coumarins from Apiaceae plants. *Rec. Nat. Prod.* **2023**, *17*, 867–877.
22. Orhan, I.E.; Tosun, F.; Senol Deniz, F.S.; Eren, G.; Mihoğlugil, F.; Akalgan, D.; Miski, M. Butyrylcholinesterase-inhibiting natural coumarin molecules as potential leads. *Phytochem. Lett.* **2021**, *44*, 48–54. [[CrossRef](#)]
23. Çiçek Kaya, A.; Özbek, H.; Yuca, H.; Yılmaz, G.; Bingöl, Z.; Kazaz, C.; Gülçin, İ.; Güvenalp, Z. Phytochemical content and enzyme inhibitory effect of *Heptaptera triquetra* (Vent.) Tutin fruit against acetylcholinesterase and carbonic anhydrase I and II isoenzymes. *Chem. Pap.* **2023**, *77*, 5829–5837. [[CrossRef](#)]
24. Collu, M. *Endocannabinoid System Modulation by Natural Products from Ancient Medicinal Plants*; University of Cagliari: Cagliari, Italy, 2019.
25. Baccari, W.; Saidi, I.; Filali, I.; Znati, M.; Lazrag, H.; Tounsi, M.; Marchal, A.; Waffo-Teguo, P.; Ben Jannet, H. Semi-synthesis, α -amylase inhibition, and kinetic and molecular docking studies of arylidene-based sesquiterpene coumarins isolated from *Ferula tunetana* Pomel ex Batt. *RSC Adv.* **2024**, *14*, 4654–4665. [[CrossRef](#)]
26. Özbek, H.; Güvenalp, Z.; Yılmaz, G.; Yerdelen, K.Ö.; Kazaz, C.; Demirezer, Ö.L. In vitro anticholinesterase activity and molecular docking studies of coumarin derivatives isolated from roots of *Heptaptera cilicica*. *Med. Chem. Res.* **2018**, *27*, 538–545. [[CrossRef](#)]

27. Iranshahi, M.; Kalategi, F.; Rezaee, R.; Shahverdi, A.R.; Ito, C.; Furukawa, H.; Tokuda, H.; Itoigawa, M. Cancer Chemopreventive Activity of Terpenoid Coumarins from *Ferula* Species. *Planta Med.* **2008**, *74*, 147–150. [CrossRef] [PubMed]
28. Shahverdi, A.R.; Saadat, F.; Khorramizadeh, M.R.; Iranshahi, M.; Khoshayand, M.R. Two matrix metalloproteinases inhibitors from *Ferula persica* var. *persica*. *Phytomedicine* **2006**, *13*, 712–717. [CrossRef]
29. Wang, J.; Huo, X.; Wang, H.; Dong, A.; Zheng, Q.; Si, J. Undescribed sesquiterpene coumarins from the aerial parts of *Ferula sinkiangensis* and their anti-inflammatory activities in lipopolysaccharide-stimulated RAW 264.7 macrophages. *Phytochemistry* **2023**, *210*, 113664. [CrossRef] [PubMed]
30. Alam, M.; Khan, A.; Wadood, A.; Bashir, S.; Aman, A.; Farooq, U.; Khan, F.A.; Mabood, F.; Hussain, J.; Samiullah; et al. Bioassay-guided isolation of urease inhibitors from *Ferula narthex* Boiss. *S. Afr. J. Bot.* **2019**, *120*, 247–252. [CrossRef]
31. Fazly Bazzaz, B.S.; Iranshahi, M.; Naderinasab, M.; Hajian, S.; Sabeti, Z.; Masumi, E. Evaluation of the effects of galbanic acid from *Ferula szowitsiana* and coniferol from *F. badrakema*, as modulators of multi-drug resistance in clinical isolates of *Escherichia coli* and *Staphylococcus aureus*. *Res. Pharm. Sci.* **2010**, *5*, 21–28.
32. Bashir, S.; Alam, M.; Adhikari, A.; Shrestha, R.L.; Yousuf, S.; Ahmad, B.; Parveen, S.; Aman, A.; Iqbal Choudhary, M. New antileishmanial sesquiterpene coumarins from *Ferula narthex* Boiss. *Phytochem. Lett.* **2014**, *9*, 46–50. [CrossRef]
33. Lee, C.-L.; Chiang, L.-C.; Cheng, L.-H.; Liaw, C.-C.; Abd El-Razek, M.H.; Chang, F.-R.; Wu, Y.-C. Influenza A (H₁N₁) Antiviral and Cytotoxic Agents from *Ferula assa-foetida*. *J. Nat. Prod.* **2009**, *72*, 1568–1572. [CrossRef]
34. Valiahdi, S.M.; Iranshahi, M.; Sahebkar, A. Cytotoxic activities of phytochemicals from *Ferula* species. *DARU J. Pharm. Sci.* **2013**, *21*, 39. [CrossRef]
35. Rafatpanah, H.; Golizadeh, M.; Mahdifar, M.; Mahdavi, S.; Iranshahi, M.; Rassouli, F.B. Conferone, a coumarin from *Ferula flabelliloba*, induced toxic effects on adult T-cell leukemia/lymphoma cells. *Int. J. Immunopathol. Pharmacol.* **2023**, *37*, 03946320231197592. [CrossRef]
36. Aydogan, F.; Baykan, S.; Soliman, G.A.; Yusufoglu, H.; Bedir, E. Evaluation of the potential aphrodisiac activity of sesquiterpenoids from roots of *Ferula huber-morathii* Peşmen in male rats. *J. Ethnopharmacol.* **2020**, *257*, 112868. [CrossRef]
37. Miski, M.; Kürkcüoğlu, M.; İçsan, G.; Göger, F.; Tosun, F. Biological Activities of the Essential Oil, Fruit and Root Extracts of *Ferula drudeana* Korovin. *Planta Med.* **2013**, *79*, PN30. [CrossRef]
38. Ghoran, S.H.; Atabaki, V.; Babaei, E.; Olfatkah, S.R.; Dusek, M.; Eigner, V.; Soltani, A.; Khalaji, A.D. Isolation, spectroscopic characterization, X-ray, theoretical studies as well as in vitro cytotoxicity of samarcandin. *Bioorg. Chem.* **2016**, *66*, 27–32. [CrossRef] [PubMed]
39. NCI Samarcandin Yeast Assay Results. Available online: <https://pubchem.ncbi.nlm.nih.gov/compound/5459231#section=Biological-Test-Results> (accessed on 18 February 2025).
40. Dapiaggi, F.; Pieraccini, S.; Potenza, D.; Vasile, F.; Podlipnik, Č. Chapter 9—Designing Antiviral Substances Targeting the Ebola Virus Viral Protein 24. In *Emerging and Reemerging Viral Pathogens*; Ennaji, M.M., Ed.; Academic Press: Cambridge, MA, USA, 2020; pp. 147–177.
41. Setlur, A.S.; Naik, S.Y.; Skariyachan, S. Herbal Lead as Ideal Bioactive Compounds Against Probable Drug Targets of Ebola Virus in Comparison with Known Chemical Analogue: A Computational Drug Discovery Perspective. *Interdiscip. Sci. Comput. Life Sci.* **2017**, *9*, 254–277. [CrossRef] [PubMed]
42. Erfani, F.; Farhadi, F.; Iranshahi, M.; Boozari, M. Evaluation of the Anti-diabetic Activity of Purified Compounds of *Ferula assafoetida* by in vitro and in silico Methods. *Nat. Prod. Commun.* **2024**, *19*, 1934578X241257125. [CrossRef]
43. Kamoldinov, K.; Li, J.; Eshbakova, K.; Sagdullaev, S.; Xu, G.; Zhou, Y.; Li, J.; Aisa, H.A. Sesquiterpene coumarins from *Ferula samarkandica* Korovin and their bioactivity. *Phytochemistry* **2021**, *187*, 112705. [CrossRef]
44. Nueraihemaiti, M.; Deng, Z.; Kamoldinov, K.; Chao, N.; Habasi, M.; Aisa, H.A. The Anti-Vitiligo Effects of Feshurin In Vitro from *Ferula samarcandica* and the Mechanism of Action. *Pharmaceutics* **2024**, *17*, 1252. [CrossRef]
45. Soltani, F.; Mosaffa, F.; Iranshahi, M.; Karimi, G.; Malekaneh, M.; Haghighi, F.; Behravan, J. Evaluation of antigenotoxicity effects of umbelliprenin on human peripheral lymphocytes exposed to oxidative stress. *Cell Biol. Toxicol.* **2009**, *25*, 291–296. [CrossRef]
46. Iranshahi, M.; Askari, M.; Sahebkar, A.; Hadjipavlou, L.D. Evaluation of antioxidant, anti-inflammatory and lipoxigenase inhibitory activities of the prenylated coumarin umbelliprenin. *DARU J. Pharm. Sci.* **2009**, *17*, 99–103.
47. Shahzadi, I.; Ali, Z.; Baek, S.H.; Mirza, B.; Ahn, K.S. Assessment of the Antitumor Potential of Umbelliprenin, a Naturally Occurring Sesquiterpene Coumarin. *Biomedicines* **2020**, *8*, 126. [CrossRef]
48. Shakeri, A.; Milad, I.; Iranshahi, M. Biological properties and molecular targets of umbelliprenin—A mini-review. *J. Asian Nat. Prod. Res.* **2014**, *16*, 884–889. [CrossRef] [PubMed]
49. Eruçar, F.M.; Senadeera, S.P.D.; Wilson, J.A.; Goncharova, E.; Beutler, J.A.; Miski, M. Novel Cytotoxic Sesquiterpene Coumarin Ethers and Sulfur-Containing Compounds from the Roots of *Ferula turcica*. *Molecules* **2023**, *28*, 5733. [CrossRef] [PubMed]
50. Edalatian Tavakoli, S.; Motavalizadehkakhky, A.; Homayouni Tabrizi, M.; Mehrzad, J.; Zhiani, R. Study of the anti-cancer activity of a mesoporous silica nanoparticle surface coated with polydopamine loaded with umbelliprenin. *Sci. Rep.* **2024**, *14*, 11450. [CrossRef] [PubMed]

51. Fiorito, S.; Epifano, F.; Preziuso, F.; Cacciatore, I.; di Stefano, A.; Taddeo, V.A.; de Medina, P.; Genovese, S. Natural oxyprenylated coumarins are modulators of melanogenesis. *Eur. J. Med. Chem.* **2018**, *152*, 274–282. [\[CrossRef\]](#)
52. Hashemzaei, M.; Dousti, T.; Tsarouhas, K.; Bagheri, G.; Nikolouzakakis, T.K.; Rezaee, R.; Shakraki, J. Effect of umbelliprenin on blood pressure in high-fat diet hypertensive rats. *Farmacia* **2020**, *68*, 447–452. [\[CrossRef\]](#)
53. Majnooni, M.B.; Fakhri, S.; Smeriglio, A.; Trombetta, D.; Croley, C.R.; Bhattacharyya, P.; Sobarzo-Sánchez, E.; Farzaei, M.H.; Bishayee, A. Antiangiogenic Effects of Coumarins against Cancer: From Chemistry to Medicine. *Molecules* **2019**, *24*, 4278. [\[CrossRef\]](#)
54. Rashidi, M.; Khalilnezhad, A.; Amani, D.; Jamshidi, H.; Muhammadnejad, A.; Bazi, A.; Ziai, S.A. Umbelliprenin shows antitumor, antiangiogenesis, antimetastatic, anti-inflammatory, and immunostimulatory activities in 4T1 tumor-bearing Balb/c mice. *J. Cell. Physiol.* **2018**, *233*, 8908–8918. [\[CrossRef\]](#)
55. Rashidi, M.; Bazi, A.; Ahmadzadeh, A.; Romeo, O.; Rezaei-Matehkolaei, A.; Abastabar, M.; Haghani, I.; Mirzaei, S. The growth inhibitory and apoptotic effects of umbelliprenin in a mouse model of systemic candidiasis. *J. Appl. Microbiol.* **2023**, *134*, 1x201. [\[CrossRef\]](#)
56. Wang, H.; Liu, Y.; Wang, Y.; Xu, T.; Xia, G.; Huang, X. Umbelliprenin induces autophagy and apoptosis while inhibits cancer cell stemness in pancreatic cancer cells. *Cancer Med.* **2023**, *12*, 15277–15288. [\[CrossRef\]](#)
57. Hajheidari, N.; Lorigooini, Z.; Mohseni, R.; Amini-Khoei, H. Umbelliprenin attenuates comorbid behavioral disorders in acetic acid-induced colitis in mice: Mechanistic insights into hippocampal oxidative stress and neuroinflammation. *Naunyn-Schmiedeberg's Arch. Pharmacol.* **2025**, *398*, 2039–2051. [\[CrossRef\]](#)
58. Joveini, S.; Yarmohammadi, F.; Iranshahi, M.; Nikpoor, A.R.; Askari, V.R.; Attaranzadeh, A.; Etemad, L.; Taherzadeh, Z. Distinct therapeutic effects of auraptene and umbelliprenin on TNF- α and IL-17 levels in a murine model of chronic inflammation. *Heliyon* **2024**, *10*, e40731. [\[CrossRef\]](#) [\[PubMed\]](#)
59. Pavlović, I.; Petrović, S.; Milenković, M.; Stanojković, T.; Nikolić, D.; Krnić, A.; Niketić, M. Antimicrobial and Cytotoxic Activity of Extracts of *Ferula heuffelii* Griseb. ex Heuff. and Its Metabolites. *Chem. Biodivers.* **2015**, *12*, 1585–1594. [\[CrossRef\]](#)
60. Liu, Y.-L.; Cao, Y.-G.; Niu, Y.; Zheng, Y.-J.; Chen, X.; Ren, Y.-J.; Fan, X.-L.; Li, X.-D.; Ma, X.-Y.; Zheng, X.-K.; et al. Diarylpentanooids and phenylpropanoids from the roots of *Anthriscus sylvestris* (L.) Hoffm. *Phytochemistry* **2023**, *216*, 113865. [\[CrossRef\]](#)
61. Harmatha, J.; Nawrot, J. Insect feeding deterrent activity of lignans and related phenylpropanoids with a methylenedioxyphenyl (piperonyl) structure moiety. *Entomol. Exp. Appl.* **2002**, *104*, 51–60. [\[CrossRef\]](#)
62. Zheng, G.Q.; Kenney, P.M.; Lam, L.K.T. Myristicin: A potential cancer chemopreventive agent from parsley leaf oil. *J. Agric. Food Chem.* **1992**, *40*, 107–110. [\[CrossRef\]](#)
63. Lee, J.Y.; Park, W. Anti-Inflammatory Effect of Myristicin on RAW 264.7 Macrophages Stimulated with Polyinosinic-Polycytidylic Acid. *Molecules* **2011**, *16*, 7132–7142. [\[CrossRef\]](#) [\[PubMed\]](#)
64. Nilawati, A.; Atmajaningtyas, A.T.J.; Ansory, H.M. *The Influence of Myristicin Lost in Myristica fragrans Volatile Oils to Antimicrobial Activity Against B. subtilis, E. coli and S. aureus*; Atlantis Press: Amsterdam, The Netherlands, 2020; pp. 143–145.
65. Morita, T.; Jinno, K.; Kawagishi, H.; Arimoto, Y.; Suganuma, H.; Inakuma, T.; Sugiyama, K. Hepatoprotective Effect of Myristicin from Nutmeg (*Myristica fragrans*) on Lipopolysaccharide/d-Galactosamine-Induced Liver Injury. *J. Agric. Food Chem.* **2003**, *51*, 1560–1565. [\[CrossRef\]](#)
66. Zhao, Q.; Liu, C.; Shen, X.; Xiao, L.; Wang, H.; Liu, P.; Wang, L.; Xu, H. Cytoprotective effects of myristicin against hypoxia-induced apoptosis and endoplasmic reticulum stress in rat dorsal root ganglion neurons. *Mol. Med. Rep.* **2017**, *15*, 2280–2288. [\[CrossRef\]](#)
67. Qiburi, Q.; Ganbold, T.; Bao, Q.; Da, M.; Aoqier, A.; Temuqile, T.; Baigude, H. Bioactive components of ethnomedicine Eerdun Wurile regulate the transcription of pro-inflammatory cytokines in microglia. *J. Ethnopharmacol.* **2020**, *246*, 112241. [\[CrossRef\]](#)
68. Carvalho, A.A.; Andrade, L.N.; de Sousa, É.B.V.; de Sousa, D.P. Antitumor Phenylpropanoids Found in Essential Oils. *Biomed. Res. Int.* **2015**, *2015*, 392674. [\[CrossRef\]](#)
69. Pandey, R.; Mahar, R.; Hasanain, M.; Shukla, S.K.; Sarkar, J.; Rameshkumar, K.B.; Kumar, B. Rapid screening and quantitative determination of bioactive compounds from fruit extracts of *Myristica* species and their in vitro antiproliferative activity. *Food Chem.* **2016**, *211*, 483–493. [\[CrossRef\]](#)
70. Abou-Elnaga, Z.S. Insecticidal bioactivity of eco-friendly plant origin chemicals against *Culex pipiens* and *Aedes aegypti* (Diptera: Culicidae). *J. Entomol. Zool. Stud.* **2014**, *2*, 340–347.
71. Fonseca, V.J.A.; Castro dos Santos, S.; Carneiro, J.N.P.; dos Santos, A.T.L.; de Freitas, M.A.; de Carvalho, N.K.G.; dos Santos Silva, F.; dos Santos, A.G.; Meneses, A.V.S.; Farias, N.S.; et al. Characterization and analysis of the bioactivity of the *Piper rivinoides* Kunth essential oil and its components myristicin and elemicin, against opportunistic fungal pathogens. *Microb. Pathog.* **2025**, *199*, 107242. [\[CrossRef\]](#) [\[PubMed\]](#)
72. Sufina Nazar, S.; Ayyappan, J.P. Mechanistic evaluation of myristicin on apoptosis and cell cycle regulation in breast cancer cells. *J. Biochem. Mol. Toxicol.* **2024**, *38*, e23740. [\[CrossRef\]](#)

73. Seneme, E.F.; dos Santos, D.C.; Silva, E.M.R.; Franco, Y.E.M.; Longato, G.B. Pharmacological and Therapeutic Potential of Myristicin: A Literature Review. *Molecules* **2021**, *26*, 5914. [[CrossRef](#)] [[PubMed](#)]
74. Skehan, P.; Storeng, R.; Scudiero, D.; Monks, A.; McMahon, J.; Vistica, D.; Warren, J.T.; Bokesch, H.; Kenney, S.; Boyd, M.R. New colorimetric cytotoxicity assay for anticancer-drug screening. *J. Natl. Cancer Inst.* **1990**, *82*, 1107–1112. [[CrossRef](#)]
75. Rintoul, R.C.; Rassl, D.M.; Gittins, J.; Marciniak, S.J.; Mesoban, K.c. MesobanK UK: An international mesothelioma bioresource. *Thorax* **2016**, *71*, 380–382. [[CrossRef](#)]
76. Pruett, N.; Singh, A.; Shankar, A.; Schrump, D.S.; Hoang, C.D. Normal mesothelial cell lines newly derived from human pleural biopsy explants. *Am. J. Physiol.-Lung Cell. Mol. Physiol.* **2020**, *319*, L652–L660. [[CrossRef](#)]
77. Tosun, F.; Göger, F.; İşcan, G.; Kürkçüoğlu, M.; Kuran, F.K.; Miski, M. Biological activities of the fruit essential oil, fruit, and root extracts of *Ferula drudeana* Korovin, the putative Anatolian ecotype of the silphion plant. *Plants* **2023**, *12*, 830. [[CrossRef](#)]
78. Altia, M.; Anbarasan, P. Regioselective Synthesis of 2,3-Disubstituted Indoles via Interrupted Heyns Rearrangement Involving C-C Bond Cleavage. *Chem. Asian J.* **2024**, *19*, e202400731. [[CrossRef](#)]

Disclaimer/Publisher’s Note: The statements, opinions and data contained in all publications are solely those of the individual author(s) and contributor(s) and not of MDPI and/or the editor(s). MDPI and/or the editor(s) disclaim responsibility for any injury to people or property resulting from any ideas, methods, instructions or products referred to in the content.